Optical manipulation and study of single gold nanoparticles in solution

Ruijgrok, P.V.

6

Acoustic vibrations of single gold nanoparticles optically trapped in water

Abstract – We combine ultrafast pump-probe spectroscopy with optical trapping, to study homogeneous damping of the acoustic vibrations of single gold nanospheres (80 nm diameter) and nanorods (25 nm diameter by 60 nm length) in water. We find a significant particle-to-particle variation in damping times. Our results indicate that vibrational damping occurs not only by dissipation into the liquid, but also by damping mechanisms intrinsic to the particle. Our experiment opens the study of mechanisms of intrinsic mechanical dissipation in metals at frequencies 1-1000 GHz, a range that has been difficult to access thus far.

The contents of this chapter are based on:
P. V. Ruijgrok, P. Zijlstra, A. L. Tchebotareva and M. Orrit, "Damping of acoustic vibrations of single gold nanoparticles optically trapped in water", Nano Lett. **12**, 1063 (2012)

6.1 Introduction

Acoustic vibrations of nanometer scale objects provide fundamental insight into the mechanical properties of matter. Moreover, the sizes, shape and crystallinity of the nanoobjects can be controlled and their effect on the mechanical properties investigated.[152] Of particular interest are noble metal nanoparticles, that interact strongly with light due to a collective oscillation of their conduction electrons. This oscillation is known as a surface plasmon resonance, and its energy and linewidth depend on particle composition, size, shape and environment. Due to this strong interaction, acoustic vibrations can be excited and detected with far-field optical techniques[153–156] down to very small particles sizes ($\sim$ 1 nm) and high vibration frequencies ($\sim$ 1 THz).[157] Besides fundamental interest, knowledge about mechanical properties of nanoparticles is important for applications where vibrating nanostructures are employed as ultra sensitive mass sensors.[158–161] For these applications often low damping is desired.

In experimental studies on nanoparticles thus far it has been particularly difficult to extract information about damping of mechanical vibrations. Most experiments have been performed on ensembles of particles,[36] resulting in an inhomogeneous broadening that dominates the observed damping time. This broadening arises because even the best synthesis methods produce samples with a distribution of sizes and shapes and therefore a distribution of vibration frequencies. In some very specific cases, ensemble-averaged homogeneous damping times have been extracted from measurements,[162,163] but these experiments require assumptions on how the ensemble-averaged optical response is related to the width and form of the distribution of particle sizes and shapes. Recently, it has been demonstrated that mechanical vibrations can also be observed for individual metal nanoparticles immobilized on a substrate, by performing pump-probe spectroscopy with the nanoparticles in the focal spot of a high numerical aperture microscope objective.[164–173] As inhomogeneous broadening is absent in these experiments, the homogeneous damping times are directly observed and were found to be significantly longer than the damping times observed in ensemble experiments. Single-particle experiments consistently show a large particle-to-particle variation of damping times, that has been attributed to variations in the mechanical coupling of the individual nanoparticles to the environment.[165,167–169,173] Quantitative comparison to theory in this geometry remains challenging, as the local environment is inhomogeneous due to the presence of the substrate. Additionally, the coupling of the particle to the substrate may depend on small

variations in the particle shape and capping layer, and vary from particle to particle.

A possible approach to investigate the mechanisms of mechanical damping on the nanometer length scale is to perform measurements on single particles in a homogeneous environment that can be modeled theoretically, such as a liquid. The techniques to measure acoustic vibrations on single particles thus far were not compatible with measurements in liquid, as the particle needs to be immobilized in the focal volume of the microscope for the entire duration of the pump-probe measurement, on the order of minutes. In a liquid, however, the particle quickly diffuses out of the focal volume, typically on a millisecond timescale in water.

Here, we report on the first observations of the acoustical vibrations of single gold nanoparticles in a homogeneous liquid environment, for nanospheres of 80 nm diameter and nanorods of 25 nm diameter and 60 nm length. We confine the nanoparticle to the focal volume of a high-numerical-aperture-objective with an optical trap in water. We use an infrared single-beam trap, with a wavelength far in the red wing of the plasmon resonance of the gold nanoparticles.[74,75] In this geometry, laser-induced heating is minimized, while the optical forces are large enough to achieve stable trapping of gold nanoparticles with diameters down to $\sim$10 nm,[76] up to periods of several hours for the nanoparticles used in this study.[174] We measure the acoustic vibration of the nanoparticles in the optical trap with a pump-probe spectroscopy setup as done in previous single-particle experiments, with the foci of the pump and probe beams overlapped with the trap focus. We directly observe the homogeneous damping time of the vibration, which we compare to established theory for the damping of the vibrations of an elastic sphere in a homogeneous liquid environment.[53,175–178] We consistently observe a lower quality factor of the vibration than predicted by theory. In addition, we observe a large particle-to-particle variation of the quality factor for both nanospheres and nanorods in water, similar to that previously observed for single nanoparticles on solid substrates. Our results indicate that intrinsic mechanisms within the gold nanoparticle itself are significant contributors to the damping.

6.2 Methods

Acoustic vibrations of individual nanoparticles were measured by time-resolved absorption with the ultra-fast pump-probe setup shown schematically

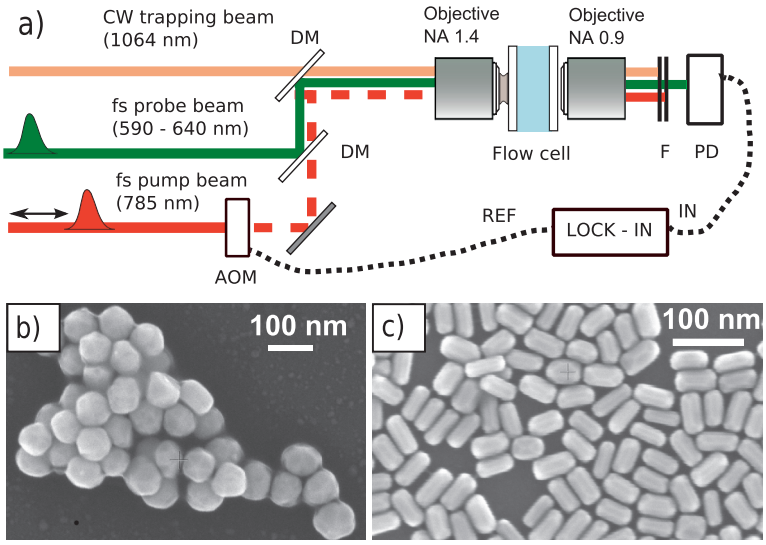

Figure 6.1: a) Schematic of the optical setup. The infrared cw trapping beam (1064 nm) is focused by a high-numerical-aperture objective into water in a flow cell, where single gold nanoparticles can be trapped for extended periods, up to several hours. Acoustic vibrations of the gold nanoparticles are investigated by a time-resolved transmission setup, consisting of femtosecond pulsed pump (785 nm) and probe (tunable 590-640 nm) beams with a variable delay, focused at the trap focus. AOM, acousto-optical modulator; DM, dichroic mirror; PD, photodiode; F, optical filters. b) Scanning electron micrograph of the gold nanospheres (80 nm diameter), and c) of gold nanorods (25 nm width and 60 nm length).

in Figure 6.1 (a), as described earlier.[166,170] Acoustic vibrations were excited with pulses from a Ti:sapphire laser with repetition rate 76 MHz (785 nm, $\sim$ 300 fs pulse length) and probed by the frequency-doubled output of an Optical Parametric Oscillator (tunable 590 nm - 640 nm, 350 fs pulse length). The intensity of the pump beam is modulated by an acousto-optical modulator at a frequency around 400 kHz. The transmitted intensity of the probe beam is recorded with a fast Si-PIN photodiode, and a lock-in amplifier extracts the small change of the detected probe intensity $\delta\mathcal{T}$ at the modulation frequency. We construct a vibration trace of the nanoparticle by recording $\delta\mathcal{T}(t)$ as function of the time delay t between pump and probe pulses, controlled using a mechanical delay stage. The wavelength of the probe beam is tuned to be close to the half maximum on either side of the plasmon resonance of the gold nanoparticles, where changes of the plasmon wavelength

are most sensitively observed.

The gold nanoparticles were held in water with a single-beam gradient optical trap.[174] The optical trap was formed by a near-infrared cw beam (1064 nm) focused by a high-numerical-aperture microscope objective, 10-20 μm away from the surface of a coverslip. To reduce spherical aberrations caused by the index mismatch between glass and water, the incoming beams were made slightly convergent.[174] Pump and probe foci were spatially overlapped with the trap focus by maximizing the pump-probe signal of a single gold nanoparticle. To confirm the presence of only a single rod in the trap, we recorded scattering spectra by collecting the backscattered white light from a Xenon lamp, on the CCD camera of a spectrometer.[174] Pump and probe pulses were kept below 10 ± 3 pJ and 0.2 ± 0.05 pJ respectively (corresponding to pulse fluences of about 4 mJ cm^{-2} and 0.2 mJ cm^{-2}). For these powers, no melting or reshaping of the nanorods was observed, as judged by a measurement of the scattering spectra before and after the measurements.

We investigated the acoustic vibrations of optically trapped nanoparticles from a sample of commercially available, roughly spherical gold nanoparticles (British Biocell International) of 80 ± 0.7 nm nominal diameter (sample standard deviation 8%) and gold nanorods with a mean length of 60 ± 0.7 nm and mean width 25 ± 0.6 nm (with sample standard deviations 8% and 16% respectively, cf. electron micrographs in Fig. 6.1 (b) and Fig. 6.1 (c)). The gold nanospheres are capped by the manufacturer with a thin organic capping layer. Gold nanorods were synthesized by silver-assisted seed-mediated growth,[119] in the presence of hexadecyltrimethylammonium bromide (CTAB). Unless otherwise indicated, the rods were functionalized with thiolated polyethyleneglycol (mPEG, M_W = 5 kDa, Sigma-Alrich) to prevent aggregation in pure water. For the experiments in the optical trap, the suspensions were diluted by 3 to 4 orders of magnitude with ultra-pure water to prevent trapping of multiple particles during the duration of a measurement, up to several hours.

6.3 Damping of acoustic vibrations of optically trapped gold nanoparticles

Acoustic vibrations of single gold nanospheres

Figure 6.2 (a) shows a typical delay trace obtained on a spherical gold nanoparticle of 80 nm diameter in the optical trap. The delay trace exhibits a

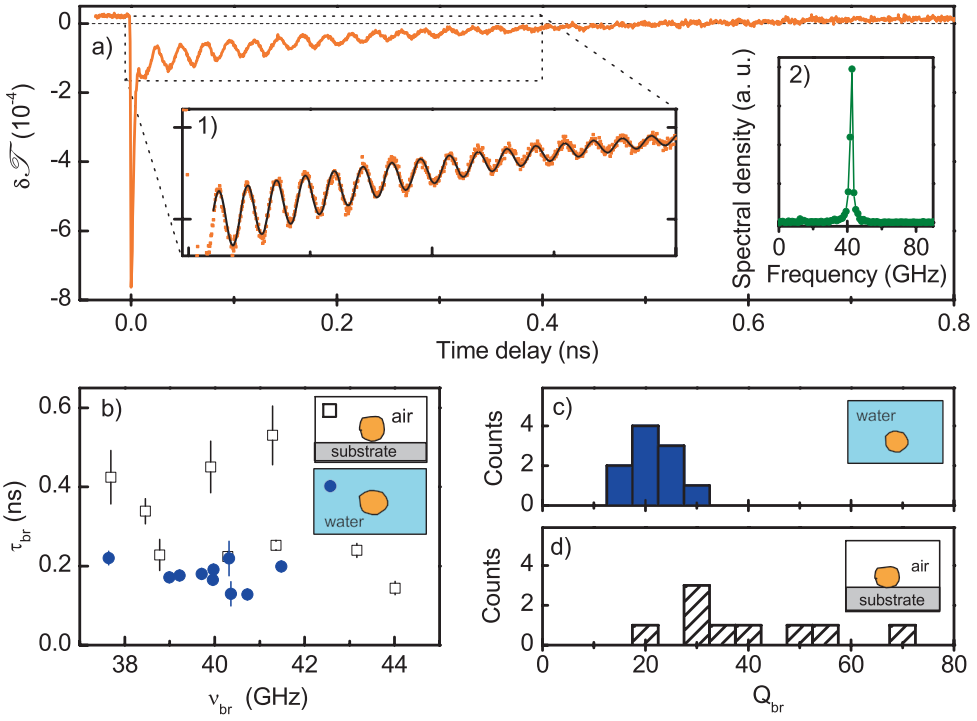

Figure 6.2: Acoustic vibrations of 80 nm diameter single gold nanospheres. (a) Trace of a single nanosphere in the optical trap in water, displaying a damped breathing mode oscillation. The probe wavelength, 595 nm, lies in the red wing of the plasmon resonance. Lock-in integration time 30 ms per point. Inset (1): Fit of eq. 6.1 to determine the frequency ν_{br} and characteristic damping time τ_{br}. Inset (2): Power spectral density of the oscillatory part of the vibrational trace. (b) Periods and damping times of the breathing mode of single particles optically trapped in water (blue solid circles) and deposited on a solid substrate (black open squares), taken on different individual particles from the same batch. (c, d): Histograms of quality factors $Q_{\mathrm{br}} = \pi \nu_{\mathrm{br}} \tau_{\mathrm{br}}$ calculated from the data in (b), for the breathing mode of single gold nanospheres in the optical trap in water (c) and for particles on a solid substrate in air (d).

short-lived peak at the temporal overlap of pump and probe pulses, and a damped oscillation and slow decay on a longer timescale. The spike at short times is caused by the heating of the electron gas by the laser pulse, leading to a broadening and shift of the plasmon resonance. The energy of the electron gas is transferred to the lattice in a few picoseconds, and dissipated into the water in several hundred picoseconds. The pump laser pulse excites an acoustic vibration of the particle by two mechanisms,[179] first by the Fermi pressure of the hot electron gas, and second due to the thermal expansion of the heated lattice, both occurring on a timescale much shorter then the natural oscillation frequencies of the particles. The elastic vibration modes of a sphere are labeled in Lamb's theory[180] by two integers, n, the harmonic order, and l, the angular momentum number. As the laser-induced excitation mechanism is spherically symmetric, mainly the spherically symmetric fundamental breathing mode $(n, l) = (0, 0)$ of the sphere is excited. This mode is detected through modulation of the particle's volume, which shifts the plasmon resonance periodically. The measured delay trace displays mainly the fundamental breathing mode, seen in the Fourier transform in the inset of Figure 6.2 (a). For some particles, weak traces of higher order modes were detected (see Section 6.4, Figure 6.4). The zoomed trace in Figure 6.2 (a) displays the initial part of the oscillation, fitted with a sum of damped oscillating terms:

$$\delta\mathscr{T}(t) = A_c \exp(-t/\tau_{\text{cool}}) + \sum_k A_k \exp(-t/\tau_k)\cos(2\pi\nu_k t - \phi_k) \qquad (6.1)$$

where the sum is over the number of damped oscillation modes, with characteristic decay time τ_k, frequency ν_k, phase ϕ_k and A_c and A_k are proportionality constants. For the spheres, only the breathing mode $k = \text{br}$ contributes. The near-exponential decay with characteristic time t_{cool} describes the effect of particle cooling and of the accompanying heating of the environment on the plasmon resonance of the particle.[181] The particle's temperature should decay as $t^{-3/2}$ on long timescales because of heat diffusion in bulk water.[182,183]

Vibration frequencies and damping times of the fundamental breathing mode of 10 individual nanospheres in the optical trap are shown as the blue solid circles in Figure 6.2 (b). The measured frequencies around 40 GHz are in good agreement with Lamb's theory for the breathing mode of an elastic sphere,[52] with the elastic constants of isotropic bulk gold. The distribution of vibration frequencies is in good agreement with the distribution of sizes in the sample. Importantly, the observed damping times of the vibration are

Nanoparticle	Mode	ν (GHz)	Q (measured)	Q_{fluid} (theory)		$Q_{\text{intrinsic}}$ (calc.)
				visc.	w. o. visc.	
Sphere (N = 10)	Breathing	40 ± 0.3 (3 %)	22 ± 1.5 (17 %)	52.5	54	40 ± 4 (29 %)
Rod (N = 7)	Breathing	73 ± 0.7 (3 %)	30 ± 1.5 (16 %)	50.5	54	89 ± 10 (36 %)
	Extensional	12 ± 0.2 (5 %)	19 ± 1.7 (24 %)	n.a.	n.a.	n.a

Table 6.1: Measured quality factors Q and frequencies ν of optically trapped single gold particles in water, nanospheres (80 nm diameter) and single-crystal nanorods (25 nm diameter, 60 nm length). Calculated breathing quality factors Q_{fluid} for damping by water according to the model by Saviot *et al*.[178] The model includes sound radiation and damping by bulk and shear viscosities. The model is evaluated for water at 30 °C in the presence (visc.) and in absence (w. o. visc.) of viscous damping, see Table S 4 Supporting Information. These values provide lower and upper bounds for Q_{fluid} in the experiment, where the water viscosity is reduced due to the elevated temperature of particle in the trap ($\approx 80 - 100$ °C). The nanorod breathing quality factor Q_{fluid} was taken equal to that of a sphere with the same breathing frequency (diameter 40 nm). The model does not apply to the extensional mode of the rods. $Q_{\text{intrinsic}}$ was calculated from 6.2, with Q_{fluid} for viscous water. Each parameter is specified by the mean $\pm$ standard error. Values in brackets indicate the standard deviation of all single particle measurements.

more widely distributed, varying by a factor of two on the investigated particles, even though they don't interact with a substrate, and they are embedded in the same environment. To facilitate the comparison of particles with different sizes and vibration frequencies, we characterize the damping by the quality factor Q of the vibration, given as $Q = 2\pi\nu_k\tau_k/2$.[171,184] We have plotted a histogram of quality factors obtained from the data of Fig. 6.2 (b) in Fig. 6.2 (c), where we observe an average $\langle Q_{\text{br}} \rangle = 22 \pm 1.5$. The spread in quality factors (standard deviation 17%, see Table 6.1) is largely determined by the spread in the damping times of the vibration.

Our measured quality factors can be directly compared to the theory of damping of vibrations of an elastic sphere embedded in a homogeneous isotropic elastic medium.[53,177] In this model, the damping is attributed to radiation of sound waves into the medium surrounding the particle. The magnitude of the damping is governed by the mismatch between acoustic impedances of the particle and the environment material, given as $Z = \rho v_L$ for longitudinal plane waves, where ρ is the material density, and v_L is the longitudinal speed of sound. For the breathing mode of a gold sphere in water, this theory predicts a quality factor $Q = 54$.[177] This value is significantly larger than the experimentally observed values, indicating that additional damping

mechanisms are present. We have estimated the effect of viscous damping for the breathing mode vibration of a gold particle of 80 nm diameter following the calculation of Saviot *et al*.[178] and found a minor correction, yielding $Q_{\text{fluid}} = 52.5$ (see Table 6.1) for the overall quality factor expected in water.

The large difference with the measured Q indicates that other dissipation mechanisms intrinsic to the particle are at work, e.g., dissipation in the organic capping layer covering the particles, or internal friction due to the anelastic properties of gold itself. The total damping rate will be the sum of the damping rates due to the various mechanisms, so that the total quality factor Q can be written as

$$Q^{-1} = Q_{\text{fluid}}^{-1} + Q_{\text{intrinsic}}^{-1} \tag{6.2}$$

where $Q_{\text{intrinsic}}$ represents all intrinsic damping mechanisms. Here, Q_{fluid} can be reliably estimated, because the particles are embedded in a well defined homogeneous environment. From the average measured quality factor $\langle Q_{\text{br}} \rangle$ and the calculated $Q_{\text{fluid}} = 52.5$, we find from our experiment $\langle Q_{\text{intrinsic}} \rangle = 40 \pm 4$.

In our experiment we find not only the average damping rate, but also the variation from particle to particle, providing valuable information on the damping mechanisms on the nanoscale. In particular, the broad distribution of quality factors (we find $16 < Q_{\text{br}} < 28$) indicates that those dissipation mechanisms are sensitive to particle-to-particle structure variations, as opposed to mechanisms sensitive mostly to bulk material properties of the particles. Taking $Q_{\text{fluid}} = 52.5$, the lowest and highest measured quality factors in the experiment correspond to $23 < Q_{\text{intr}} < 60$, respectively.

To relate our results on single gold nanoparticles trapped in water to measurements performed on single particles on a substrate,[165,167–169,173] we compare to previous measurements from our group[170] on the breathing mode of single 80 nm gold nanospheres supported on a solid substrate, surrounded by air, see Fig. 6.2 (b, d). Again, a broad distribution of damping times was found, resulting in a distribution of quality factors ranging from 20 to about 70, with a mean $\langle Q_{\text{br}} \rangle = 33 \pm 5.3$ (standard deviation 40 %). Interestingly, the average quality factor for particles on a substrate in air is higher than for those trapped in water. Moreover, we note that both the average value $\langle Q_{\text{br}} \rangle$ and its distribution are close to the values of $Q_{\text{intrinsic}}$ deduced for particles in water (see Table 6.1). This observation suggests that the gold nanospheres in air are only weakly coupled to the solid substrate, and that the observed damping time is dominated by intrinsic damping. Therefore, our results suggest a new interpretation of the broad distributions of damping times observed consis-

tently in all single-particle measurements to date. These distributions reflect inhomogeneity in intrinsic dampings, rather than variations in mechanical coupling to the substrate.

Acoustic vibrations of single gold nanorods

Whereas gold nanospheres may have a variety of crystal structures - single crystalline, multiple twinned or irregular[185–187] - gold nanorods synthesized by seed-mediated growth in the presence of silver ions are known to be single crystals, with a growth direction along the [1 0 0] direction.[188–190] If damping mechanisms related to crystal defects or grain boundaries contribute dominantly to the intrinsic damping, we expect to observe higher quality factors for single crystal rods than for polycrystalline spheres.

A representative vibration trace of an optically trapped single gold nanorod is shown in Figure 6.3 (a). Two oscillation modes are detected, as highlighted in the Fourier transform of the trace in the inset, and attributed to the breathing (about 75 GHz) and extensional (about 10 GHz) modes.[191] The breathing mode involves radial expansion and depends on both the bulk and shear elasticity moduli, whereas the extensional mode involves an axial expansion combined with a radial contraction, and probes the Young's modulus along the long axis of the rod.[191]

The frequencies and damping times of the breathing and extensional modes of 7 nanorods in the optical trap are shown in Fig. 6.3 (b)-(c). For comparison, we also plotted the measured frequencies and damping times of single nanorods of similar sizes and aspect ratios immobilized on a clean silica substrate in air, from previous work.[166] For the nanorods in water, the frequency ratio of the two vibration modes is strongly correlated to their aspect ratio deduced from the measured longitudinal plasmon resonance resonance (See Section 6.5, Fig. 6.5).

The quality factors of the breathing and extensional modes are shown in the scatter plot Fig. 6.3 (d). The average quality factor of the breathing mode measured on the trapped nanorods is $\langle Q_{br} \rangle = 30 \pm 1.5$. We expect that the damping rate of the breathing mode due to radiation of sound waves for our short aspect ratio nanorods will be close to the value predicted for spheres. We therefore estimate $Q_{\text{fluid}} = 50.5$ by calculating the damping for a sphere with the same vibration frequency as the rods, see Table 6.1. Using this value we find $\langle Q_{\text{int}} \rangle = 84 \pm 10$, indeed significantly higher than for spheres. The Q-factors we find for gold nanorods suggest that crystal structure is an important factor in the intrinsic damping. The extensional mode of the rods has

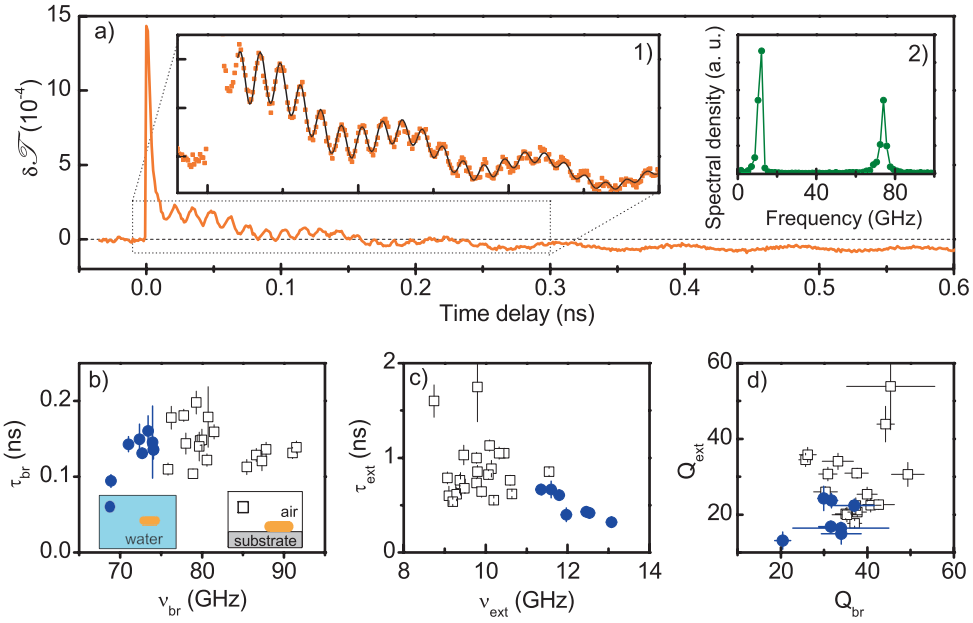

Figure 6.3: Acoustic vibrations of single gold nanorods. (a) Vibration trace of a single 25 nm × 60 nm gold nanorod, optically trapped in water. The probe wavelength, 610 nm, lies in the blue wing of the plasmon resonance. Inset (1): zoom of a part of the trace, fitted with a sum of two damped oscillations and slow cooling. The fit gives the frequencies $\nu_{\mathrm{br}}, \nu_{\mathrm{ext}}$ and damping times $\tau_{\mathrm{br}}, \tau_{\mathrm{ext}}$ of the breathing and extensional modes. Lock-in integration time 30 ms per point. Inset (2): Power spectral density of the oscillatory part of the vibrational trace. (b-d) Parameters of the vibrations of single gold nanorods, optically trapped in water (blue solid circles, sample of 25 nm × 60 nm nanorods) and immobilized on a solid substrate in air (black open squares, sample of 30 nm × 90 nm rods). (b),(c) Scatter plots of the damping time τ_{br},τ_{ext} versus vibration frequency ν_{br},ν_{ext}, for the breathing and extensional modes. (d) Scatter plot of the quality factor $Q = 2\pi\nu\tau/2$ of the breathing mode (Q_{br}) versus that of the extensional mode Q_{ext}. Error bars are the fit inaccuracies.

an average quality factor of $\langle Q \rangle = 19 \pm 1.7$, lower than that of the breathing mode. As the extensional mode involves a large shear displacement, it may be more sensitive to viscous damping by the water. A quantitative analysis of the damping of the extensional mode requires extensive numerical modeling and is beyond the scope of this paper. As was observed for the spheres, the quality factors of the nanorods are broadly distributed.

To determine the contribution of the capping layer of the nanorods to the

damping, we have attempted a measurement of the damping rates of gold nanorods stabilized by CTAB. CTAB is expected to form a bilayer of $\sim$4 nm thickness on the surface on the gold nanorod.[133] We found that trapping was less stable in this configuration. Thus far, we measured 2 nanorods in CTAB, and found damping rates similar to those of the mPEG-coated nanorods.

Discussion

Our measurements of acoustic damping of gold nanoparticles in water indicate that dissipation into the surrounding liquid and intrinsic dissipation in the nanoparticle are of similar magnitude. This result is surprising, as in most of the previous literature the damping of nanoparticle vibrations was assumed to arise mainly from radiation of sound waves into the surrounding medium. Recently, Pelton et al. have provided experimental evidence that intrinsic damping mechanisms cannot be neglected for ensembles of gold bipyramids.[163] Their measurement of the homogeneous damping time of the extensional vibration mode in various liquids was consistent with an intrinsic quality factor $\langle Q_{\text{intrinsic}} \rangle = 25 \pm 3$, in the same range as our results on the breathing mode of gold nanospheres ($\langle Q_{\text{intrinsic}} \rangle = 37 \pm 4$) and gold nanorods $\langle Q_{\text{intrinsic}} \rangle = 84 \pm 10$.

Our measurements on single particles reveal a significant variation in the damping rates from particle to particle, indicating that a significant fraction of the intrinsic damping is caused by dissipation mechanisms that are sensitive to particle-to-particle variations in shape, crystal structure or defects. In the following we discuss several possible contributions.

Crystal defects contribute to dissipation, and variations in structural defects may contribute to a particle-to-particle variation of damping rates. Indeed, as gold nanorods have less defects than spheres, we expect and observe higher quality factors for nanorods than for spheres. It is known that as-synthesized rods are single crystals, without stacking faults, twins or dislocations,[189] but we cannot exclude the presence of internal defects on the basis of our experimental results. Although rods have fewer defects than spheres, variations in number of defects could still lead to the observed particle-to-particle variation of damping rates. In addition, a crystal defect common to all nanoparticles is their surface itself. Surface atoms are more mobile than bulk atoms,[185] providing additional channels for dissipation. Due to the large surface-to-volume ratio of the particle, the dynamics at the surface may provide a significant contribution to the total damping. Finally, for nanorods the damping rate could be influenced by the silver atoms used during rod syn-

thesis. Gold nanorods grown by the silver-assisted seed-mediated route[119] contain 2-3% silver (by number of atoms),[192] possibly opening additional dissipation channels.

The organic molecules capping nanoparticles may also contribute to the damping, and capping layer structure variations may also lead to particle-to-particle variations of the damping rate. For the extensional vibration mode of gold bi-pyramids,[163] Pelton et al. found that the capping layer of the particles may be responsible for up to 30% of the intrinsic damping. We therefore do not expect the thin organic capping layer to contribute more than 30% to the damping of the 80 nm gold spheres. For the 25 nm diameter gold nanorods the capping layer could contribute more to the damping, because of the larger surface-to-volume ratio and higher vibration frequency. However, preliminary experiments showed no big difference in damping rates between CTAB and PEG capping layers.

Our experiment opens the possibility to study the mechanisms of mechanical dissipation in metals, at frequencies in the range of 1 GHz - 1 THz. Whereas damping mechanisms in macroscopic structures have been well studied,[193] much less is known about dissipation mechanisms at these high vibration frequencies. Quality factors in the range 10^3 up to 10^5 were found for poly-crystalline gold nanoresonators with vibration frequencies in the 10 MHz-100 MHz range.[194,195] At temperatures from 1 mK to $\sim$100 K, a dominant part of damping was attributed to dislocations. The vibration frequencies in nanoparticles are much higher however, and different mechanisms may be dominant. Studies on macroscopic samples indicate that metals have higher intrinsic losses than dielectrics, due to their conduction electrons.[196] At room temperature and for frequencies of several GHz and above, intrinsic losses are high for both metals and dielectrics, as known from microwave ultrasonics.[196] In fact, losses are typically so high that they are difficult to measure accurately in macroscopic samples, and not much experimental work has been done in this regime.[196,197] Measurements on damping of acoustic vibrations in nanoparticles provides a novel access to explore this area. This range is particularly interesting as both electron and phonon relaxation times are comparable to the period of the sound wave, and mean free paths are comparable to the particle size.[196] As in experiments on macroscopic samples, it may be possible to probe internal friction in metal nanoparticles, as a function of frequency, temperature, crystal structure and crystal orientation. Of particular value would be the correlation of vibrational measurements on a single nanoparticle to its exact morphology obtained by high-resolution transmission electron microscopy.

6.4 Higher order vibrational modes of gold nanospheres

In our experiment, the vibrational response of the trapped gold nanospheres is dominated by the breathing mode. However, weak signatures of other vibration modes are detected on some particles. The vibration modes of an elastic sphere have been first calculated by Lamb more than a century ago.[52] The vibration modes in Lamb's theory are labeled by two integers, n, the harmonic order, i.e. the number of radial nodes, and l, the angular momentum number, representing the angular dependence of the mode.

Fig. 6.4 (a) shows a vibrational spectrum of a trapped sphere that displayed several vibration frequencies. Besides the fundamental breathing mode $(n,l) = (0,0)$ at $\Omega_{0,0} = 38.8\,\mathrm{GHz}$, vibration modes are detected at 84 GHz and 126 GHz. These frequencies are close to the values calculated in Lamb's theory for the first higher order radial modes of a 80 nm gold sphere[180] with a free boundary condition, taking the bulk elastic constants of gold. For the first higher order radial modes $(1,0)$ and $(2,0)$ the calculated frequencies are $\Omega_{1,0} = 2.1\,\Omega_{0,0}$ and $\Omega_{2,0} = 3.18\,\Omega_{0,0}$. The $(1,0)$ radial mode was detected for 3 out of the 10 investigated single gold spheres. The excitation and detection of this mode appears robust: if the mode was found for a particular sphere, it was observed in each of several (2-5) consecutive vibrational spectra acquired on that particle in the optical trap, over a time span of up to 30 minutes. The second order radial mode $(2,0)$ was clearly observed for 2 out the 3 the particles that displayed the $(1,0)$ mode, but in both cases appeared in only one trace out of a series of vibrational traces acquired on the particle.

Some particles (3 out of 10) displayed a weak vibration mode with a frequency around 0.3 times the breathing mode frequency. A vibrational spectrum of a such a particle is shown in Fig. 6.4 (b). The mode at 12.5 GHz is possibly the non-spherically symmetric $(n,l) = (0,2)$ mode, corresponding to a uniaxial cigar-to-pancake deformation of the spheres. The excitation of this mode is not expected for spheres, embedded in an isotropic environment and subject to a spherically symmetric excitation mechanism. However, the ellipsoidal vibration mode can be excited in slightly elongated particles,[170] where the spherical symmetry is broken.

6.5 Vibration modes of gold nanorods

Figure 6.5 displays the scaling of the breathing mode frequency ν_{br} to the extensional mode frequency ν_{ext} measured on single gold nanorods in an opti-

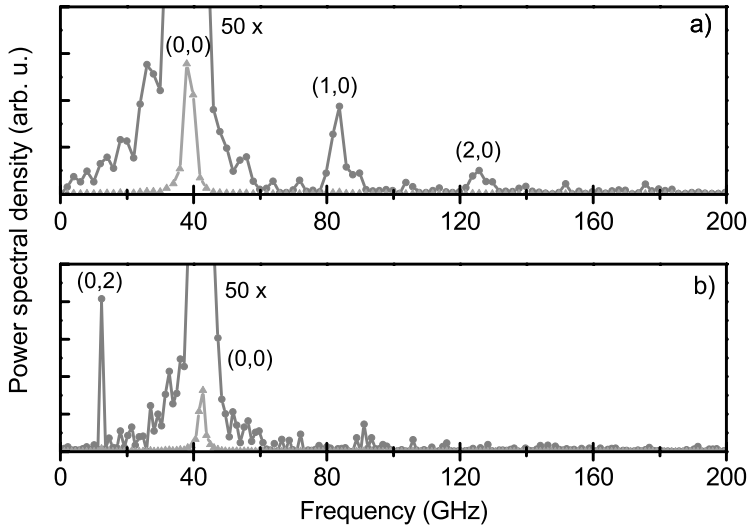

Figure 6.4: Vibration modes of single 80 nm gold spheres optically trapped in water. Vibrational spectra are dominated by the fundamental breathing mode $\Omega_{0,0}$ around 40 GHz, but weak traces of other vibrational modes are detected. (a) Vibrational spectrum of a sphere with a breathing mode at $\Omega_{0,0} = 38.8$ GHz. Weak traces of the higher order radial modes $(n,l) = (1,0)$ at $\Omega_{1,0}$ (84 GHz, $2.16 \times \Omega_{0,0}$) and $(n,l) = (2,0)$ at $\Omega_{2,0}$ (126 GHz, $3.25 \times \Omega_{0,0}$) are detected. (b) Vibrational spectrum of a sphere with a breathing mode at $\Omega_{2,0} = 42.4$ GHz. An additional vibration mode at 12.5 GHz ($0.29 \times \Omega_{0,0}$) is attributed to the $(0,2)$ ellipsoidal deformation mode.

cal trap in water. Data on the same nanorods is reported in Fig. 6.3 in Section 6.3. In addition to the data on the 7 PEG-coated rods in Section 6.3, data on 2 nanorods stabilized in CTAB are included.

It is expected that the frequency ratio $\nu_{\mathrm{br}}/\nu_{\mathrm{ext}}$ is proportional to the aspect ratio of the rod.[191] In our experiment we can estimate the aspect ratio for each individual nanorod in the trap from the longitudinal plasmon resonance λ_{L}, obtained from the rods scattering spectrum. Here, we approximate $\mathrm{AR} = (\lambda_{\mathrm{L}} - 410)/85$, with λ_{L} in units of nm, by calculation of the plasmon resonance of a gold ellipsoidal particle in water, in the dipole limit. The data points in Figure 6.5 all fall on a horizontal line, indicating that the frequency ratio $\nu_{\mathrm{br}}/\nu_{\mathrm{ext}}$ is strongly correlated to the rods aspect ratio. The graph also displays the theoretical values calculated for a polycrystalline rod[191] (dashed line, $\nu_{\mathrm{br}}/\nu_{\mathrm{ext}} = 2.32 \times \mathrm{AR}$) and for a single crystalline rod[166] with its long axis along the [1 0 0] direction (dotted line, $\nu_{\mathrm{br}}/\nu_{\mathrm{ext}} = 3.24 \times \mathrm{AR}$). It appears that the data are closer to the value expected for polycrystalline rods than for sin-

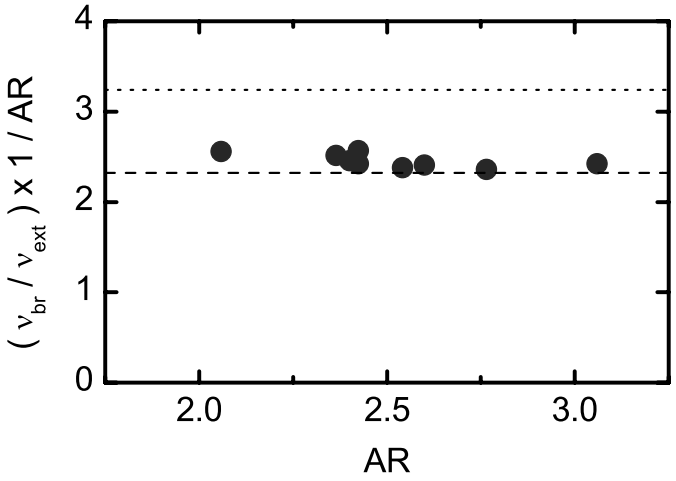

Figure 6.5: Ratio of breathing mode and extensional mode frequencies of optically trapped nanorods, as function of aspect ratio. The aspect ratio was deduced from the measured wavelength of the longitudinal plasmon resonance λ_R via AR $= (\lambda_R - 410)/85$, with λ_R in nm. Dashed line: theoretical value for a gold nanorod with polycrystalline elastic constants.[166,191] Dotted line: theoretical value for a single crystalline rod, with the long axis of the rod in the the [1 0 0] direction.

gle crystal rods. However, this attribution depends critically on the absolute value of the aspect ratio. It is difficult to obtain an accurate absolute relation between the aspect ratio of the rod and its longitudinal plasmon resonance. Calculated values of the resonance depend sensitively on the exact shape of the tip of the rod, and on the exact thickness and structure of the capping layer, parameters that are not known with high precision for the individual rods in our experiment. Therefore, we do yet draw quantitative conclusions from the absolute value of the proportionality constant found in Fig. 6.5. The assumption of a linear relation between aspect ratio and plasmon resonance is more robust, so that our data nevertheless provides evidence for a strong correlation between aspect ratio and vibration frequency.

To come to a quantitative conclusion about the scaling of vibration mode frequencies in gold nanorods, it would be necessary to determine the exact aspect ratio of each individual nanorod in the trap by electron microscopy on the nanorod, as was done previously for nanorods immobilized on a substrate.[166]

6.6 Conclusions

We have measured for the first time acoustic vibrations of single gold nanoparticles in an optical trap in water. Our approach directly provides the homogeneous damping time of the vibrations of the nanoparticle, in an isotropic liquid environment. We find that vibrations of the nanoparticles are damped not only by dissipation into the environment, but that damping mechanisms intrinsic to the particle must be taken into account. This intrinsic damping leads to ensemble-averaged quality factors in the range $\langle Q_{\text{intrinsic}} \rangle = 40 \pm 4$ (for 80 nm nanospheres) to $\langle Q_{\text{intrinsic}} \rangle = 84 \pm 10$ (for 25 nm $\times$ 60 nm nanorods). Intrinsic quality factors vary largely for individual particles (standard deviations $\sim$30 % and $\sim$40 % for spheres and rods, respectively). This particle-to-particle variation provides a signature of mechanisms of intrinsic damping that are sensitive to nanometer scale variations in particle structure. Our results are the first step in the investigation of mechanisms of mechanical dissipation in metals in the frequency range 1-1000 GHz, a range that has been difficult to access so far.